European Journal of Radiology 116 (2019) 47–54

Contents lists available at ScienceDirect

European Journal of Radiology

journal homepage: www.elsevier.com/locate/ejrad

Evaluation of hepatic iron concentration heterogeneities using the MRI R2* mapping method

Jean Mazé[a], Guillaume Vesselle[a], Guillaume Herpe[a], Samy Boucebci[a], Christine Silvain[b], Pierre Ingrand[c], Jean-Pierre Tasu[a,*]

[a] Imaging Department, CHU de Poitiers, 2 Rue de la milétrie, 86000 CHU de Poitiers, France
[b] Hepatology Department, CHU de Poitiers, 2 Rue de la milétrie, 86000 CHU de Poitiers, France
[c] Inserm U619, CHU de Poitiers et University of Poitiers, Rue de la milétrie, 86000 CHU de Poitiers, France

ARTICLE INFO

Keywords:
Iron
Liver
MRI
Quantification
R2* mapping

ABSTRACT

Objective: To measure hepatic iron concentration (HIC) heterogeneities using a magnetic resonance R2* mapping method.

Patients and methods: Ninety-four patients with suspected hepatic iron overload and 10 volunteers were included prospectively. A multi-echo R2* sequence with fat saturation and with three post-processing fitting methods (a single exponential decay model with or without truncation, SED and SEDt, and a constant offset model, COS) was compared to a signal intensity ratio method (SIR), considered as the reference. HIC heterogeneity was evaluated from R2* mapping after placing a ROI on each liver segment.

Results: A strong linear correlation between SIR and R2* methods using the SEDt and COS models was observed (r = 0.973 and 0.955, respectively). Volunteers and patient liver variabilities, quantified by mean intra-liver standard deviation (SD) were 1.58 μmol/g (mean range 5.06 μmol/g) and 4.73 μmol/g (mean range 19.08 μmol/g), respectively. For the patient group, the highest HIC was observed in the IVth segment. Heterogeneity increased for patients with an HIC > 60 μmol/g (mean intra-liver SD = 13.90 μmol/g; mean range = 50.60 μmol/g).

Conclusion: This study is the first to demonstrate *in vivo* HIC heterogeneities using whole-liver mapping analysis. These preliminary results require confirmation through further studies, but might be useful in cases of single ROI analysis.

1. Introduction

Magnetic resonance imaging (MRI) is currently the most widely available technique used to evaluate liver iron load [1]. The underlying mechanism is that the MR relaxation time of hydrogen nuclei decreases with increasing amounts of iron. Two main techniques have been developed, both of which are based-on T1, T2, and T2* relaxation time shortening if there is iron content in the liver:; 1—a semi-quantitative method, using a signal intensity ratio (SIR) from a region of interest (ROI) between the liver and a reference tissue that does not accumulate iron (commonly the paraspinous muscles). This method is well-established and reproducible [2] and studies have demonstrated its robustness versus liver biopsies, the gold standard method; and 2—a quantitative method that measures T2* (or less frequently T2) decay rates using various echo times [3]. As T2* has a negative relationship with hepatic iron concentration (HIC), it is commonly converted into R2* according to the relationship R2* = 1000/T2*; thus, the relaxation rate becomes directly proportional to HIC. T2* measurements can be obtained from signal averages in the ROI or on a pixel-by-pixel basis, which results in liver iron overload maps [4]. This second technique presents different limitations due to a lack of standardization of the different models used for T2* curve-fitting and for the applied echo times (TEs). In addition, a quick decrease in the T2* signal leads to an underestimation of iron quantification, particularly in cases of high HIC [5].

There are only a few studies comparing the accuracy of the two MR

Abbreviations: ROI, region of interest; MRI, magnetic resonance imaging; HIC, hepatic iron concentration; SED, single exponential decay model without truncation; SEDt, single exponential decay model with truncation; COS, constant offset; SIR, signal intensity ratio; TE, time of echo; FIESTA, fast imaging employing steady-state acquisition; SD, standard deviation

* Corresponding author at: Service de Radiologie, 2 rue de la milétrie, 86000 Poitiers, France.
E-mail address: jean-pierre.tasu@chu-poitiers.fr (J.-P. Tasu).

https://doi.org/10.1016/j.ejrad.2018.02.011
Received 25 October 2017; Received in revised form 5 February 2018; Accepted 9 February 2018

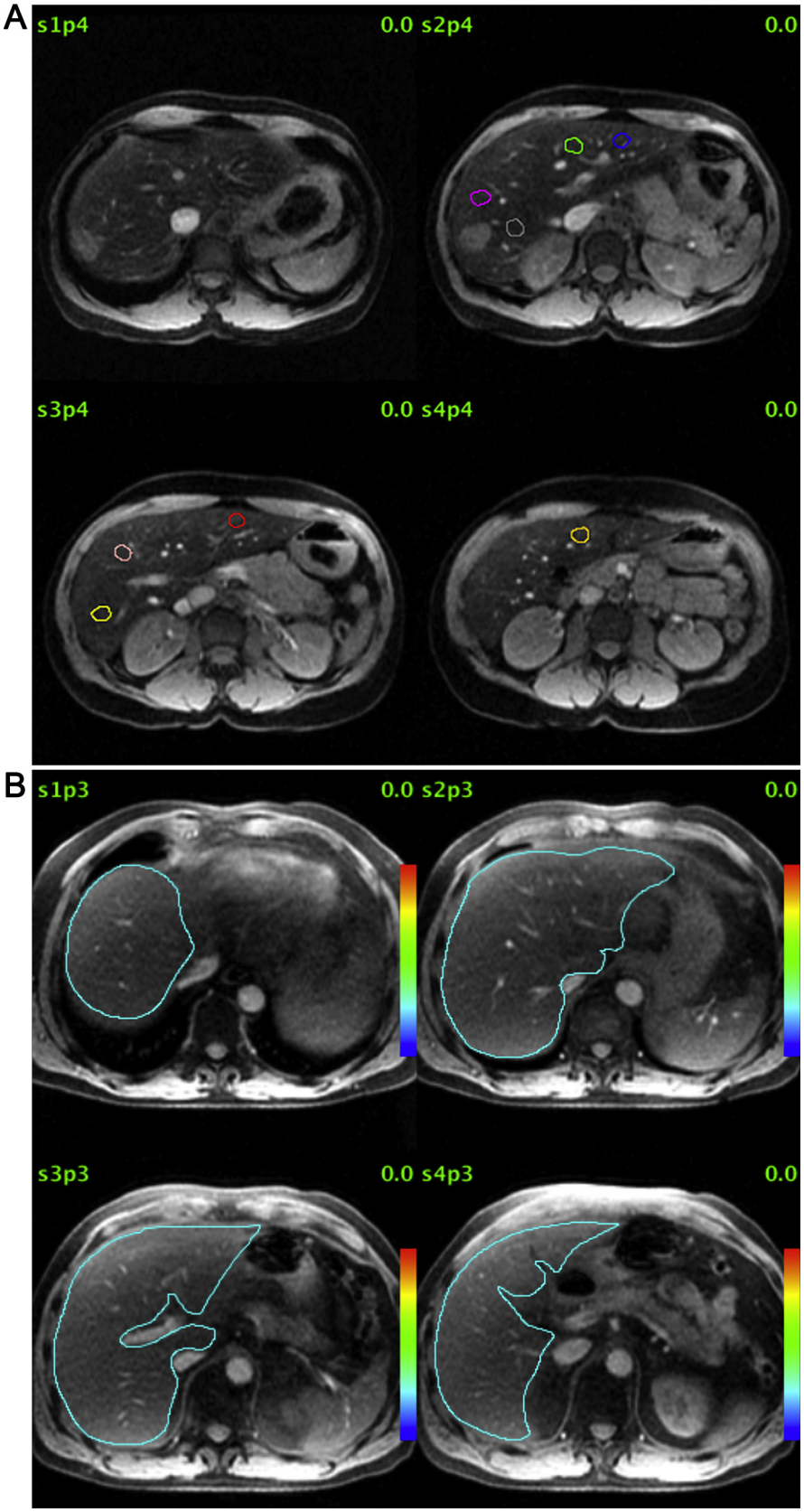

Fig. 1. Example of multi-ROI placement on the liver using the four slice multi-echo T2* sequence. In 1A, a segmental analysis. In 1B, a whole-liver analysis.

methods [6–8] and the impact of the different post-processing procedures of the R2* method [9,10]. In addition, to date, only one team has studied hepatic iron heterogeneity and those authors failed to demonstrate any variation on MRI, although this has been proven by pathological results [11].

Therefore, the purpose of this study was to evaluate HIC liver

heterogeneities from T2* mapping measurements. The different post-processing models used for T2* measurements were first compared with the SIR method used as the gold standard method.

2. Materials and methods

2.1. Patients

Over a nineteen-month period (November 2014 to May 2016), all patients who were referred for suspicion of liver iron overload and who were scheduled for a MRI examination were included prospectively. Laboratory tests were performed, at most, 10 days after the MRI examination, including a serum dosage of ferritin and an evaluation of the transferrin saturation coefficient. For patients with suspected genetic disease, a search for the C282Y and H63D mutations was performed. Noninvasive liver fibrosis tests were performed to quantify fibrosis (*fibroscan*® and *Fibrotest*®). All included patients gave their written, informed consent to participate. The local ethics committee approved the study. The privacy rights of human subjects were observed in agreement with the local laws. A group of 10 volunteers was also included. They had no history of hepatic, immunologic, or viral disease nor were they taking any medication for a genetic disease.

2.2. MRI techniques and image analysis

All examinations were performed on a 1.5 T optima MR 450 w (General Electric Healthcare, Milwaukee, USA). The protocol systematically included axial slice morphological sequences, T2 FIESTA (Fast Imaging Employing Steady-state Acquisition) and T1 in/out phases (TE 4.2 ms and 2.1 ms, respectively).

To quantify HIC using the SIR method, the Rennes University protocol proposed by Gandon et al. [12], including a T1-weighted gradient echo sequence (TR = 120 ms; TE = 4 ms; FA = 90°) and four T2-weighted breath-hold gradient echo sequences (TR = 120 ms; multiple TE = 4, 9, 14, 21 ms; FA = 20°), was used.

To quantify HIC using the R2* method, a fat-saturated multi-gradient echo sequence with 12 echo times (TE initial = 1.4 ms; TE final = 22.4 ms; delta TE = 1.9 ms; TR = 51.3 ms; FA = 25°; matrix = 224 × 160 pixels; NEX = 1; FOV = 42 × 31.5 cm) was used. During one breath-hold of 16 s, four axial hepatic slices were acquired, with a thickness of 8 mm every 10 mm, to cover each liver segment.

2.3. Post-processing

1—To quantify SIR for each sequence, three regions of interest (ROI) that contained at least 100 pixels in the right hepatic lobe and two ROIs in the paraspinous muscles on the same axial slice (total number of regions of interest = 25) were drawn. The signal intensity of each ROI was then used to obtain the HIC from the dedicated Rennes University website (http://www.radio.univ-rennes1.fr/Sources/FR/HemoCalc15.html).

2—For R2* quantification, three image analyses were performed.

First, **a single ROI** was placed on the right liver (at least 100 mm^2), in a vessel-free area, avoiding other sources of artefacts (i.e., motion). Estimation of R2* values was performed by fitting the R2* signal using three decay models: a single exponential decay model, SED (*a*), and a single exponential decay model with truncation method, SEDt (*b*). Later echo times were manually excluded so as to limit noise effects at low T2* values. The third decay model was also applied using a constant offset, COS (*c*).

Second, a **multi ROI** analysis was performed to evaluate the heterogeneous deposition of iron. A ROI with at least 100 pixels was drawn in each hepatic segment, determined according to the Couinaud classification [13]. The ROI was placed in the area of homogeneous liver on the T2* images. Considering the relatively lower signal-to-noise ratio and the influence of inferior vena cava movements, segment I was excluded from the analysis. Two ROIs were positioned in segment IV, one at the upper part (IVa) and the other at the lower part (Ivb), giving a total number of eight ROIs (Fig. 1).

Finally, a whole-liver ROI was obtained by contouring the whole liver on four axial slices, excluding major vessels. Within this large ROI, two ROIs were drawn, one in the area that showed the lowest HIC, the second in area that showed the highest HIC according to the T2* colour maps. The HIC range was computed from the difference between the highest and the lowest values. For the multi-ROI approach, the signal was fitted by a single exponential equation with a constant offset model (COS).

All R2* values from the single ROI analysis were correlated with HIC using the SIR method. SIR and R2* relaxometry methods were also compared after transformation according to the Wood's calibration algorithm when the COS method was used: Fe (mg/g) = 0.0254 × R2* + 0.202 [14]. For other R2* relaxometry methods, a second linear regression model was used: Fe (mg/g) = 0.02876 × R2* + 0.137 [3]. For both, the HIC was converted into units of μmol/g using the following formula: Fe (mg/g) = 55.845 × 10^{-3} × Fe (μmol/g).

To compare SIR and R2*, three iron levels were used [12]: no iron overload (< 36 μmol/g); mild iron overload (36–100 μmol/g); and high iron overload (> 100 μmol/g).

To evaluate liver heterogeneity from R2* mapping, four groups were defined according to R2* measures: group 1 with no iron overload (HIC < 36 μmol/g); group 2 with a mild iron overload (36 < HIC < 60 μmol/g); group 3 with an iron overload higher than 60 μmol/g; and group 4, which comprised the 10 volunteers. The mean intra-liver standard deviation (SD) and the mean range between the subgroups were compared.

Hepatic fat content was estimated based on chemical shift imaging (CSI) using T1-weighted in- and opposed-phase gradient-recalled echo (GRE) MRI sequences and the following formula: Fat fraction (FF) = 100 × (signal IP − signal OP)/2 × signal IP [15]. Fat content was considered significant if the FF was over 5%.

2.4. Statistical analysis

Intra-liver standard deviation (SD) was extracted for each subgroup. Mean intra-liver SD and the mean range were compared between the sub-groups. A linear regression model was fitted to the patient data to assess the relationship between HIC and the R2* signal. Agreement between the SIR method and T2* relaxometry was assessed by Bland Altman plots. The Kolmogorov-Smirnov test was used to assess the normality of distribution parameters. In case of deviation from the normality assumption, a logarithmic transformation was performed. Correlation between parameters was analysed using Pearson' r-correlation coefficients. A two-way analysis of variance (ANOVA) with logarithmic transformation was used to compare HIC between segments. A p value less than 0.05 was considered statistically significant. Statistical computations used SAS V9.4 and Prism V5 computer software.

3. Results

3.1. Patients and serum ferritin

Ninety-four patients (M/F: 69/25; mean age: 54.5 +/− 14.1-year-old) and 10 volunteers (M/F: 7/3; mean age: 28.2 +/− 8.2 year-old) were included during the study period. The diseases that caused iron overload were dysmetabolic hepatosiderosis syndrome (N = 54), hereditary hemochromatosis C282Y +/+ or H63D +/+ (N = 6), acute leukemia (N = 4), double heterozygous mutation C282Y +/− and H63D +/− (N = 3), sickle cell disease (N = 3), thalassemia (N = 2), and Gilbert's disease (N = 1). The cause of hyperferritinemia remained unknown for 21 patients at the time of study analysis. Fifty-five patients

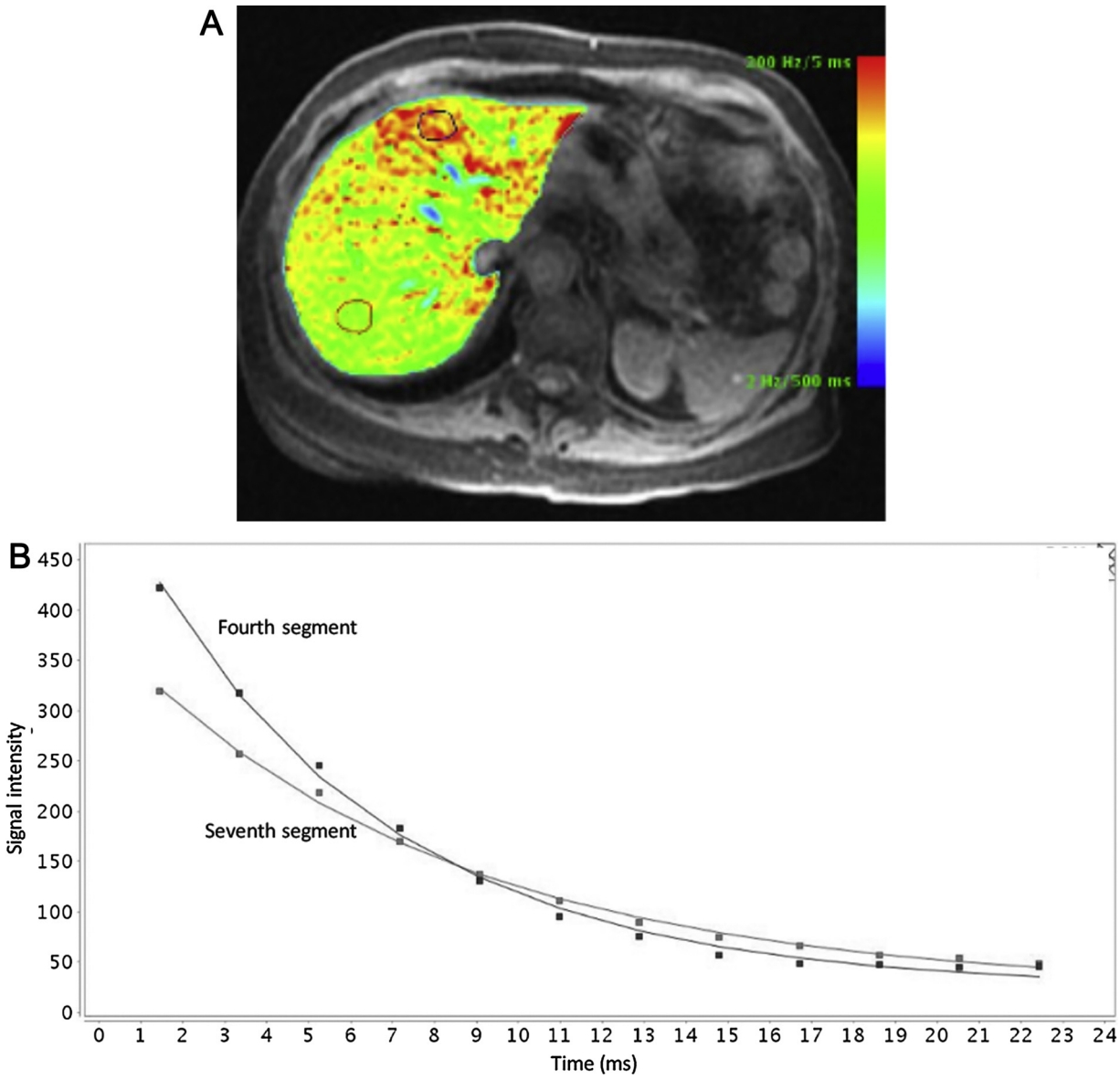

Fig. 2. A patient with a heterogeneous deposit of iron in the liver on R2* mapping. The HIC measured within ROI 1 (placed on the fourth segment) and within ROI2 (placed on the seventh segment of the liver), as illustrated in Fig. 2A, are quite different (Fig. 2B): 83 µmol/g versus 63 µmol/g, respectively.

were assessed for fibrosis stage with noninvasive tests. Sixteen subjects (29%) had significant fibrosis (stage greater than F2). Laboratory tests were performed for 78 patients (83%) at a delay of less than two months from the MR examination. Serum ferritin ranged from 13 to 3876 ng/mL (mean = 818.3 +/− 597.4 ng/mL). Fat fraction ranged from 7 to 48% (mean = 21.3%). Forty-four of 94 patients (47%) had fatty liver disease according to the 5% MR criterion (M/F = 37/7) (Fig. 2).

3.2. Single ROI analysis

For the patient group, mean hepatic iron concentration using the SIR method was 76.44 +/− 59.69 µmol/g (ranging from 5 to 350 µmol/g). Mean hepatic R2* using SED, SEDt, and COS models was 69.3 +/− 22.8 Hz, 80.8 +/− 50.7 Hz, and 95.4 +/− 62.4 Hz, respectively. Table 1 gives the main results. A strong linear relationship was observed between the SIR method and the R2* transverse relaxation rate using the truncation and offset decay models (Fig. 3). The SED model, however, was weakly correlated to the SIR results ($r = 0.657$).

Table 2 and Fig. 4 show the main results for the comparison of the SIR and R2* methods in the entire cohort. The two methods gave discordant results when stratifying the HIC according to the three levels of iron content defined for this study.

Table 1
Mean ± SD results for the patient group (N = 94) using the three decay models.

	SED	SEDt	COS
R2* (Hz)	69.3 ± 22.8	80,8 ± 50.7	95.4 ± 62.4
HIC (µmol/g)	35.2 ± 10.4	44.1 ± 26.1[a]	47.1 ± 28.4[b]
Difference SIR – R2* (µmol/g)	41.3 ± 53.4	32.4 ± 34.8	29.4 ± 33.6

[a] According to the Wood calibration curve.
[b] According to the Henninger calibration curve.

3.3. Multi-ROI analysis

3.3.1. Segmental variability

Table 3 provides the main results.

For volunteers, the HIC multi-ROI ranged from −4.73% (seg IVb) to +5.30% (seg VIII). Intra-liver variability, quantified by mean intra-

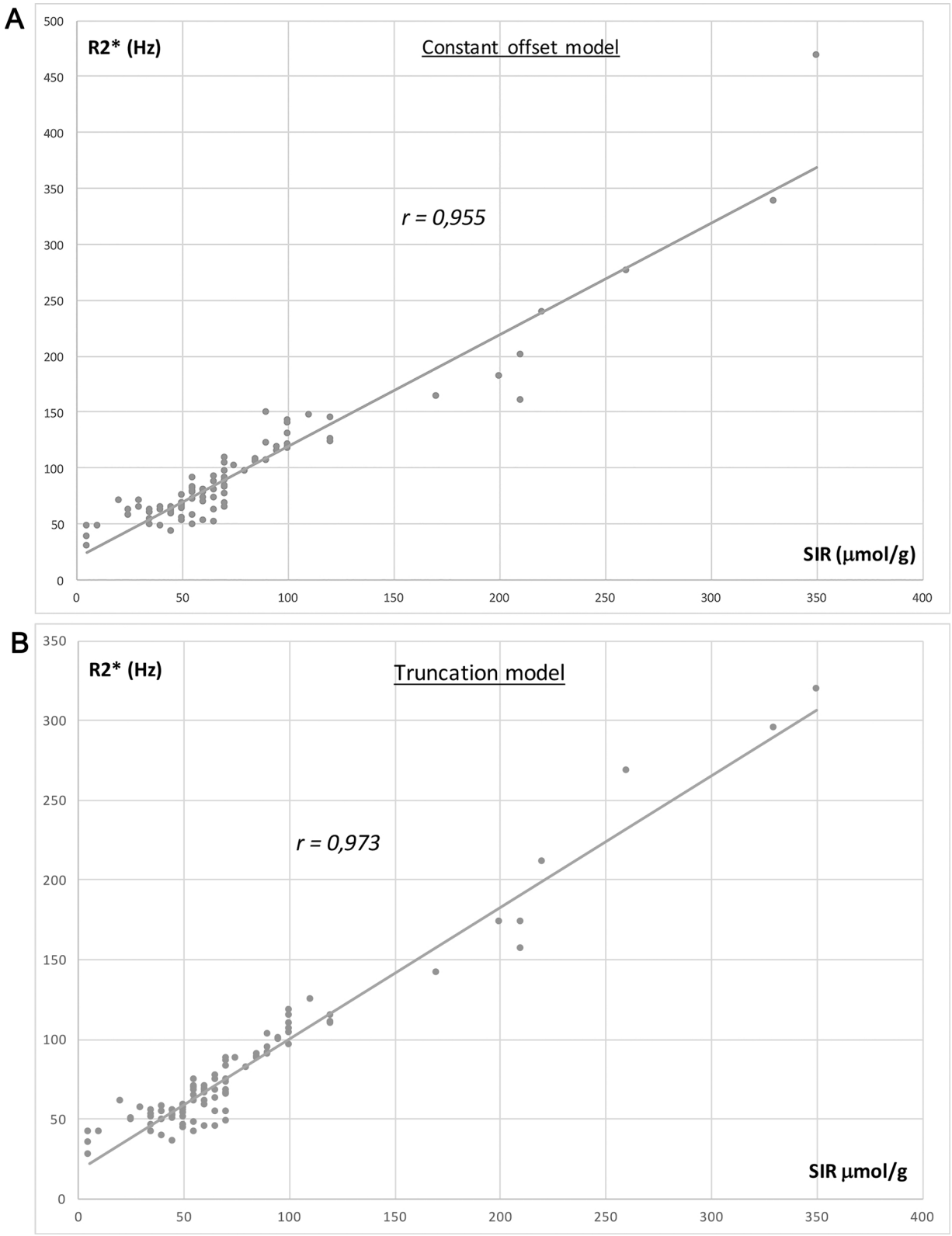

Fig. 3. Distribution of R2* values for patients with HIC heterogeneities according to the SIR method. Linear regression equations and coefficients of correlation are given on the graphs according to each model used (constant offset, 3A; truncature 3B).

liver SD and mean range, was 1.58 µmol/g (CV = 6.4%) and 5.06 µmol/g, respectively.

In the patient group, eight were excluded (N = 86) from the multi-ROI analysis because the four axial slices did not include all hepatic segments. The mean multi-ROI HIC (50.09 +/− 35.02 µmol/g) and the mean single-ROI HIC (48.38 +/− 29.33 µmol/g) were significantly different (p = .0471). For ANOVA analysis, the highest iron concentration was observed in the IVa segment (52.60 µmol/g). The mean iron concentration in segment VIII was significantly higher than the mean HIC in segments III and VI. The lowest HIC was in segment VI.

Table 2
Correlation between the SIR and the R2* relaxometry methods according to various levels of overload.

R2*	SIR			
Truncation model				
	< 36	*36–99*	*> 100*	
< 36	**23**	44	0	67
36–99	0	**19**	15	34
> 100	0	0	**3**	3
	23	63	18	**104**
Offset model				
	< 36	*36–99*	*> 100*	
< 36	**23**	27	*0*	50
36–99	0	**36**	14	50
> 100	0	0	4	4
	23	63	18	**104**

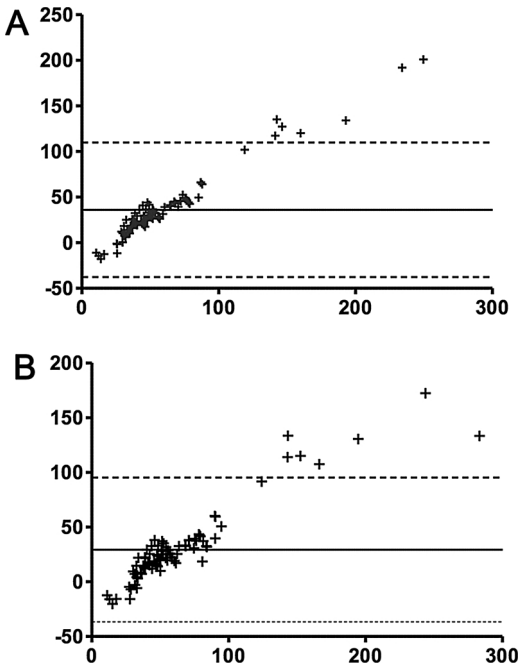

Fig. 4. Agreement between SIR and R2* methods according to Bland and Altman plots. Mean HIC as units of µmol/g is given on the abscissa and differences in SIR-R2* on the ordinate. The solid line represents the mean difference: 36 ± 37.6 µmol/g and 29.4 ± 33.6 µmol/g for the truncature (4A) and the offset models (4B), respectively.

Nineteen patients (22%) had simultaneous segments with no iron overload and mild iron overload. Three patients had segments with mild and moderate iron overload. Two patients had segments with moderate and high iron overload. Fig. 2 illustrates a case of HIC heterogeneities.

In the sub-group of patients with significant fatty liver content, iron concentrations were 38.48 +/− 11.94 µmol/g and 38.00 +/− 11.66 µmol/g, respectively, for the mean HIC single-ROI and the mean HIC multi-ROI methods (not significantly different). The highest iron concentration was detected in segment IVa, followed by segment VIII, as in the entire patient cohort.

In a group that included 18 patients with moderate-to-high overload according to the SIR method (> 100 µmol/g; mean SIR method = 167.78 µmol/g), the mean HIC single-ROI was 87.93 +/− 42.31 µmol/g and the mean HIC multi-ROI was 95.13 +/− 54.56 µmol/g. The highest mean segmental iron concentration was detected in segment IVb and the lowest mean in segment VII. The ANOVA test found significant segmental variability. The mean HIC in segments IVa, IVb, and VIII was significantly higher than the mean HIC in the other segments, except for segments II and V. The percentage of deviation of the segments from the mean HIC multi-ROI ranged from −10.43% (seg VII) to + 6.79% (seg IVb). The mean intra-liver SD was 12.44 µmol/g and the mean range was 46.07 µmol/g. CV = 13.1%.

In the sub-group of patients with significant fibrosis (N = 16), there was no significant segmental variability (p = .171).

3.3.2. *Intra-liver variability: analysis of R2* mapping (Table 4)*

For this analysis, group 1 included 43 patients with no iron overload (mean age: 52.5 +/− 13.1-year-old), group 2 were patients with mild iron overload (36 patients, mean age: 51.0 +/− 11.1-year-old), group 3 were patients with an iron overload of > 60 µmol/g (15 patients, mean age: 55.5 +/− 12.7-year-old), and the 10 volunteers (group 4). Eight patients were excluded from group 1 (multi-ROI analysis not feasible, N = 35). Significant differences (p < 0.0001) were found between each group. Mean intra-liver SDs between the sub-groups were significantly different, except between group 1 and group 4. The mean ranges between them were likewise significantly different. The highest mean intra-liver SD and range were detected in group 3 Table 4.

4. Discussion

While heterogeneity in iron liver overload is well known by pathologists, this study is the first to quantify it *in vivo* from liver R2* mapping. For this purpose, we used a specific fitting that seems accurate compared to the SIR method, and two parameters: intra-liver SD, and the range reflecting heterogeneity. Heterogeneity seems to be higher in the IVth segment in cases of higher iron deposit. In addition, variability of the iron hepatic load increases with iron content.

The heterogeneity of iron deposition has been demonstrated in different histological studies through multiple biopsies from liver transplants [16–18]. Coefficients of variation ranged from 7 to 80% and Edmond et al. observed that the SD was significantly correlated with the mean HIC [18]. What remains under discussion is the pattern of this heterogeneity. In a study by Ambu et al., [19], a preferential subcapsular accumulation was shown, and the highest iron concentrations were detected in the left lobe. However, liver biopsies provide only local sample estimates, and multiple biopsies are not applicable in clinical practice.

Multiple ROI methods or whole-liver analysis can be achieved by R2* mapping, which is accurate compared to the other widely used MR method, SIR [2,3,14,20,21]. To our knowledge, there have been only two previous studies on *in vivo* liver iron heterogeneities using R2* imaging [11,22]. In the first [11], Meloni et al. observed greater segmental variability in the healthy group with no iron liver overload, although, for moderate and high iron hepatic overload, variability was considered negligible. The authors explained these paradoxical results by magnetic susceptibility effects that accelerate T2* decay. The authors consequently proposed an algorithm to correct these susceptibility effects, which led to complete disappearance of all heterogeneities in patients and volunteers. In our healthy group, it is interesting to note that, as in the study by Meloni et al., the highest variation of HIC was found in segment VIII, followed by segment VII. But, in our study, the variations around the mean measurements were 4–5 times lower: −4.7% to + 5.3% compared to −22.9% to + 19.8%, respectively. Due to the high level of variations, Meloni et al. had to use susceptibility corrections. Conversely, our lower level of variation allowed us to apply our data without any filtration.

The second study, by Sofue et al., was centered on the reproducibility of measurements of fat fraction and iron content from R2* measurements. The authors also described small but significant variability in R2* measurements in different hepatic segments. However, the study was designed to measure only a limited number of liver segments and heterogeneity in the whole liver was not evaluated [22].

A major confounder of R2* measurements is the presence of fat, which introduces sinusoidal modulations in signal evolution [5,23].

Table 3
results according each liver segment.

	Volunteers N = 10	Patient group N = 86	HIC > 60 µmol/g[a] N = 15	HIC > 100µmol/g[b] N = 18	Steatosis N = 38
Seg II	24.84*	50.31*	104.27	96.28	***37.62**** ***(−2.23%)***
Seg III	24.05	48.99*	97.39*	91.16*	38.02*
Seg IVa	25.05*	***52.60**** ***(+5.01%)***	***109.93**** ***(+7.50%)***	101.38*	***40.03**** ***(+4.03%)***
Seg IVb	***23.35**** ***(−4.73%)***	51.16*	108.41	***101.59**** ***(+6.79%)***	38.33*
Seg V	24.05*	50.77*	107.68	100.04	38.08*
Seg VI	23.39*	***47.33**** ***(−5.51%)***	92.84*	86.22*	38.19*
Seg VII	25.55*	48.13*	***91.54**** ***(−10.48%)***	***85.21**** ***(−10.43%)***	38.53*
Seg VIII	***25.81**** ***(+5.30%)***	51.46*	106.03	99.17*	39.01
Mean HIC multi-ROI	24.51	50.09	102.26	95.13	38.48
Mean HIC single-ROI	25.27	48.38	94.80	87.93	38
Mean intra-liver SD	1.58	4.73	13.90	12.44	2,45
CV (%)	6.45%	9.44%	13.59%	13.08%	6.37%
Mean range	5.06	19.08	50.60	46.07	12.88

Mean values are presented in µmol/g. For each group, the lowest and the highest values (with% of deviation from the mean HIC multi-ROI)are shown in bold.
* Indicates $p < 0.05$ using the ANOVA test.
[a] According to R2* method.
[b] According to SIR method.

Table 4
Comparison of sub-groups with different HICs.

Sub-groups	*1*	*2*	*3*	*4*
Number of patients	35	36	15	10
Steatosis +	21	14	3	0
Mean HIC (µmol/g)	30.23	47.66	102.26	24.51
Mean intra-liver SD (µmol/g)	2.10	3.47	13.90	1.58
CV (%)	6.90	7.28	13.60	6.40
Mean range (µmol/g)	9.88	15.11	50.60	5.06

Sub-groups: 1 = HIC < 36 µmol/g; 2 = 36 < HIC < 60 µmol/g; 3 = HIC > 60 µmol/g; 4 = volunteers.

These modulations arise from the different resonance frequencies for water and lipid protons, which can affect R2* evaluation. Different post-processing techniques [24–26] have been proposed, such as acquisition of echo when fat and water components are approximately in-phase (TE increments of approximately 2 ms at 1.5T). However, this approach could be hampered by fat–fat signal interferences that limit its application in cases of high HIC. To avoid fat-water modulations, fat suppression (FS) techniques were also used [27,28], as in this work. However, both methods, in-phase acquisition and FS, might have limited application in high HIC, given that the accessible temporal range in which to evaluate fat-water modulations is restricted due to rapid signal decay [5].

In this study, the hepatic fat fraction was estimated according to CSI FF, using T1-weighted in- and opposed-phase GRE MRI sequences, the technique most commonly used in liver MR imaging [29]. There are other methods, such as spectroscopy, the reference method, which is more complex to perform routinely, and the CSI fat fraction corrected to the spleen according to Koelblinger et al. [30]. The correction provided better correlations than CSI FF on a small cohort of 35 patients, at 3T with no cases of iron overload. However, in a dysmetabolic syndrome population, such as the one in our study, in which iron deposits into the spleen are frequent, this correction should not be performed.

To evaluate liver iron content, a 3D multiecho Dixon MR sequence R2* has been recently proposed [31] and it offers several advantages, among which is that there is no need for specialized offline software or postprocessing tools. Another advantage of a 3D multiecho Dixon sequence over 2D GRE sequences, in daily clinical practice, is that fat and iron can be simultaneously assessed for the whole liver. Further studies are nevertheless required to evaluate this interesting technique for the evaluation of hepatic iron concentration heterogeneities with MRI.

Our study has several limitations. First, pathological correlations of iron and fat content were not available. Nevertheless, biopsies for these indications are currently rare, given the fact that non-invasive methods suffice for clinical care. The gold standard method used in this study was the SIR method, but SIR and T2* are not equivalent methods and this point could be debated. However, strong correlations between SIR and liver iron concentration have been widely demonstrated [2,12]. Second, there was a significant difference in terms of age between patients and volunteers and the average age in the patient group was twice that of the age in the control group, which might have influenced the results. Third, only a few of our patients had a high hepatic iron overload considering that a large majority of them were included for dysmetabolic syndrome. Our results might not be applicable for high HIC, and further studies are required. Finally, we did not assess intra- and inter-reader reproducibility. However, previous reports have demonstrated the excellent reproducibility of all the methods used here [6,32].

5. Conclusion

This study shows that liver iron concentration varies in the liver within the same patient, and that it can be evaluated using the MR T2* relaxometry method. HIC variability increases with iron content and concentrations seem to be higher in the IVth segment. Consequently, methods using a single ROI could place the ROI in this segment rather than, as is the case in current practice, in the right liver.

Guarantor

The scientific guarantor of this publication is Jean MAZE.

Conflict of interest

The authors of this manuscript declare no relationships with any companies, whose products or services may be related to the subject matter of the article.

Funding

The authors state that this work has not received any funding.

Statistics and biometry

One of the authors has significant statistical expertise (P Ingrand).

Informed consent

Written informed consent was obtained from all subjects (patients)

in this study.

Ethical approval

Institutional Review Board approval was obtained.

Study subjects or cohorts overlap

Study subject have never been previously reported.

Methodology

- prospective
- diagnostic or prognostic study
- performed at one institution

Acknowledgment

The authors would like to thank Jeffrey Arsham for his useful review of the English language.

Appendix A. Supplementary data

Supplementary data associated with this article can be found, in the online version, at https://doi.org/10.1016/j.ejrad.2018.02.011.

References

[1] C.T. Quinn, T.G. St Pierre, MRI measurements of iron load in transfusion-dependent patients: implementation challenges, and pitfalls, Pediatr. Blood Cancer 63 (2016) 773–780.
[2] J.M. Alustiza, J. Artetxe, A. Castiella, et al., MR quantification of hepatic iron concentration, Radiology 230 (2004) 479–484.
[3] B. Henninger, H. Zoller, S. Rauch, et al., R2* relaxometry for the quantification of hepatic iron overload: biopsy-based calibration and comparison with the literature, Rofo 187 (2015) 472–479.
[4] T. Yokoo, Q. Yuan, J. Senegas, A.J. Wiethoff, I. Pedrosa, Quantitative R2* MRI of the liver with rician noise models for evaluation of hepatic iron overload: simulation, phantom, and early clinical experience, J. Magn. Reson. Imaging 42 (2015) 1544–1559.
[5] A.J. Krafft, R.B. Loeffler, R. Song, et al., Does fat suppression via chemically selective saturation affect R2*-MRI for transfusional iron overload assessment? A clinical evaluation at 1.5T and 3T, Magn. Reson. Med. 76 (2016) 591–601.
[6] J.M. Virtanen, M.E. Komu, R.K. Parkkola, Quantitative liver iron measurement by magnetic resonance imaging: in vitro and in vivo assessment of the liver to muscle signal intensity and the R2* methods, Magn. Reson. Imaging 26 (2008) 1175–1182.
[7] A. Christoforidis, V. Perifanis, G. Spanos, et al., MRI assessment of liver iron content in thalassamic patients with three different protocols: comparisons and correlations, Eur. J. Haematol. 82 (2009) 388–392.
[8] S. Verlhac, M. Morel, F. Bernaudin, S. Bechet, C. Jung, M. Vasile, Liver iron overload assessment by MRI R2* relaxometry in highly transfused pediatric patients: an agreement and reproducibility study, Diagn. Interv. Imaging 96 (2015) 259–264.
[9] S.H. Ibrahim el, A.M. Khalifa, A.K. Eldaly, The influence of the analysis technique on estimating liver iron overload using magnetic resonance imaging T2* quantification, Conf. Proc. IEEE Eng. Med. Biol. Soc. 2014 (2014) 4639–4642.
[10] V. Positano, A. Pepe, M.F. Santarelli, et al., Multislice multiecho T2* cardiac magnetic resonance for the detection of heterogeneous myocardial iron distribution in thalassaemia patients, NMR Biomed. 22 (2009) 707–715.
[11] A. Meloni, A. Luciani, V. Positano, et al., Single region of interest versus multislice T2* MRI approach for the quantification of hepatic iron overload, J. Magn. Reson. Imaging 33 (2011) 348–355.
[12] Y. Gandon, D. Olivie, D. Guyader, et al., Non-invasive assessment of hepatic iron stores by MRI, Lancet 363 (2004) 357–362.
[13] S. Rutkauskas, V. Gedrimas, J. Pundzius, G. Barauskas, A. Basevicius, Clinical and anatomical basis for the classification of the structural parts of liver, Medicina (Kaunas) 42 (2006) 98–106.
[14] J.C. Wood, C. Enriquez, N. Ghugre, et al., MRI R2 and R2* mapping accurately estimates hepatic iron concentration in transfusion-dependent thalassemia and sickle cell disease patients, Blood 106 (2005) 1460–1465.
[15] H.K. Hussain, T.L. Chenevert, F.J. Londy, et al., Hepatic fat fraction: MR imaging for quantitative measurement and display–early experience, Radiology 237 (2005) 1048–1055.
[16] H.G. Kreeftenberg, B.J. Koopman, J.R. Huizenga, T. van Vilsteren, B.G. Wolthers, C.H. Gips, Measurement of iron in liver biopsies–a comparison of three analytical methods, Clin. Chim. Acta 144 (1984) 255–262.
[17] J. Ludwig, E. Hashimoto, M.K. Porayko, T.P. Moyer, W.P. Baldus, Hemosiderosis in cirrhosis: a study of 447 native livers, Gastroenterology 112 (1997) 882–888.
[18] M.J. Emond, M.P. Bronner, T.H. Carlson, M. Lin, R.F. Labbe, K.V. Kowdley, Quantitative study of the variability of hepatic iron concentrations, Clin. Chem. 45 (1999) 340–346.
[19] R. Ambu, G. Crisponi, R. Sciot, et al., Uneven hepatic iron and phosphorus distribution in beta-thalassemia, J. Hepatol. 23 (1995) 544–549.
[20] P.R. Clark, W. Chua-Anusorn, T.G. St Pierre, Proton transverse relaxation rate (R2) images of liver tissue; mapping local tissue iron concentrations with MRI [corrected], Magn. Reson. Med. 49 (2003) 572–575.
[21] C. Rose, P. Vandevenne, E. Bourgeois, N. Cambier, O. Ernst, Liver iron content assessment by routine and simple magnetic resonance imaging procedure in highly transfused patients, Eur. J. Haematol. 77 (2006) 145–149.
[22] K. Sofue, A. Mileto, B.M. Dale, X. Zhong, M.R. Bashir, Interexamination repeatability and spatial heterogeneity of liver iron and fat quantification using MRI-based multistep adaptive fitting algorithm, J. Magn. Reson. Imaging 42 (2015) 1281–1290.
[23] C.B. Sirlin, S.B. Reeder, Magnetic resonance imaging quantification of liver iron, Magn. Reson. Imaging Clin. North Am. 18 (2010) 359–381 ix.
[24] H. Yu, A. Shimakawa, C.A. McKenzie, E. Brodsky, J.H. Brittain, S.B. Reeder, Multiecho water-fat separation and simultaneous R2* estimation with multifrequency fat spectrum modeling, Magn. Reson. Med. 60 (2008) 1122–1134.
[25] A.C. Westphalen, A. Qayyum, B.M. Yeh, et al., Liver fat: effect of hepatic iron deposition on evaluation with opposed-phase MR imaging, Radiology 242 (2007) 450–455.
[26] D.P. O'Regan, M.F. Callaghan, M. Wylezinska-Arridge, et al., Liver fat content and T2*: simultaneous measurement by using breath-hold multiecho MR imaging at 3.0 T–feasibility, Radiology 247 (2008) 550–557.
[27] L. Sanches-Rocha, B. Serpa, E. Figueiredo, N. Hamerschlak, R. Baroni, Comparison between multi-echo T2* with and without fat saturation pulse for quantification of liver iron overload, Magn. Reson. Imaging 31 (2013) 1704–1708.
[28] A. Meloni, J.M. Tyszka, A. Pepe, J.C. Wood, Effect of inversion recovery fat suppression on hepatic R2* quantitation in transfusional siderosis, AJR Am. J. Roentgenol. 204 (2015) 625–629.
[29] F.H. Cassidy, T. Yokoo, L. Aganovic, et al., Fatty liver disease: MR imaging techniques for the detection and quantification of liver steatosis, Radiographics 29 (2009) 231–260.
[30] C. Koelblinger, M. Krssak, J. Maresch, et al., Hepatic steatosis assessment with 1H-spectroscopy and chemical shift imaging at 3.0T before hepatic surgery: reliable enough for making clinical decisions? Eur. J. Radiol. 81 (2012) 2990–2995.
[31] B. Henninger, H. Zoller, S. Kannengiesser, X. Zhong, W. Jaschke, C. Kremser, 3D multiecho dixon for the evaluation of hepatic iron and fat in a clinical setting, J. Magn. Reson. Imaging 46 (2017) 793–800.
[32] P. Saiviroonporn, V. Viprakasit, K. Sanpakit, J.C. Wood, R. Krittayaphong, Intersite validations of the pixel-wise method for liver R2* analysis in transfusion-dependent thalassemia patients: a more accessible and affordable diagnostic technology, Hematol. Oncol. Stem Cell Ther. 5 (2012) 91–95.